C. Das
V. Nayak
S. Raghothama
P. Balaram

Synthetic protein design: construction of a four-stranded β-sheet structure and evaluation of its integrity in methanol–water systems

Authors' affiliations:
C. Das and P. Balaram, Molecular Biophysics Unit, Indian Institute of Science, Bangalore, India.

V. Nayak and S. Raghothama, Sophisticated Instrument Facility, Indian Institute of Science, Bangalore, India.

Correspondence to:
Professor *P. Balaram*
Molecular Biophysics Unit
Indian Institute of Science
Bangalore 560012
India
Tel.: 91-80-309-2337
Fax: 91-80-360-0683 (91-80-360-0535)
E-mail: pb@mbu.iisc.ernet.in

Dates:
Received 18 February 2000
Revised 4 May 2000
Accepted 8 June 2000

To cite this article:
Das, C., Nayak, V., Raghothama, S. & Balaram, P. Synthetic protein design: construction of a four-stranded β-sheet structure and evaluation of its integrity in methanol–water systems.
J. Peptide Res., 2000, **56,** 307–317.

ISSN 1397–002X

Key words: protein design; designed β-sheet motif; synthetic peptide; conformational analysis; NMR

Abstract: The characterization of a four-stranded β-sheet structure in a designed 26-residue peptide Beta-4 is described. The sequence of Beta-4 (Arg-Gly-Thr-Ile-Lys-^{D}pro-Gly-Ile-Thr-Phe-Ala-^{D}Pro-Ala-Thr-Val-Leu-Phe-Ala-Val-^{D}Pro-Gly-Lys-Thr-Leu-Tyr-Arg) was chosen such that three strategically positioned ^{D}Pro-Xxx segments nucleate type II′ β-turns, which facilitate hairpin extension. A four-stranded β-sheet structure is determined in methanol from 500 MHz ^{1}H NMR data using a total of 100 observed NOEs, 11 dihedral restraints obtained from vicinal $J_{C\alpha H\text{-}NH}$ values and 10 hydrogen bonding constraints obtained from H/D exchange data. The observed NOEs provide strong evidence for a stable four-stranded sheet and a nonpolar cluster involving Ile^{8}, Phe^{10}, Val^{15} and Phe^{17}. Circular dichroism studies in water–methanol mixtures provide evidence for melting of the β-sheet structure at high water concentrations. NMR analysis establishes that the four-stranded sheet in Beta-4 is appreciably populated in 50% (v/v) aqueous methanol. In water, the peptide structure is disorganized, although the three β-turn nuclei appear to be maintained.

Abbreviations: CD, circular dichroism; Fmoc, 9-fluorenylmethyloxycarbonyl; HPLC, high-performance liquid chromatography; TFA, trifkuoroacetic acid; TSP, trimethylsilylpropionate.

The rational design of peptide sequences that fold into predetermined secondary and super secondary structures provides a critical test of our understanding of the stereochemical principles that control polypeptide chain folding and the interactions that determine the spatial arrangement

of modules of secondary structures. Major targets of *de novo* design of protein structures have been helical bundles (1,2) and β-sheets (3–6). Although design strategies have been pursued for over a decade there have been relatively few successes in structurally characterizing synthetic mimics for protein structures (7–9). The design of helical structures (10) and their assembly into bundles (11–14) has progressed considerably, while β-sheets have proved less amenable to synthetic design.

Several recent reports have described the successful design of stable β-hairpin structures (15–23) and three-stranded β-sheets in synthetic peptides (24–28). A key element in the design of β-hairpins is the nucleation of tight reverse turns of the appropriate stereochemistry. A valuable analysis of protein crystal structures in the mid-1980s by Thornton and colleagues provided the important insight that hairpins in proteins accommodate the 'enantiomeric' β-turns (type I′ and II′) as the pivotal central segment (29–31). The type I′ and II′ β-turn conformations [Ramachandran angles (ϕ, ψ) at the '*i*+1' and '*i*+2' residues for these turn types are: type I′ +60°, +30° and +90°, 0°; type II′ +60°, −120° and −80°, 0°] (32) require that the residue at the '*i*+1' position must adopt *positive* values of the dihedral angle ϕ, a feature generally inconsistent with the occurrence of L-amino acids at this position. In designed peptides, this is readily achieved by incorporation of the ^{D}Pro residue in which the constraint of pyrrolidine ring formation restricts $\phi_{D\text{-}Pro}$ to $\approx +60 \pm 20°$. The use of ^{D}Pro-Xxx segments positioned centrally in synthetic peptide sequences to nucleate β-hairpin formation has been demonstrated (15–19). L-Asn residues have also been used as potential turn nucleators (20,23) because of their high propensity to form left-handed helical (α_L) conformations (33,34) with $\phi \approx +60°$, $\psi \approx +30°$, which are stereochemically acceptable at both positions in type I′ β-turns. Comparitive studies establish that ^{D}Pro-Gly segments are superior to Asn-Gly segments in hairpin nucleation (35). An important feature of hairpin design is the wide tolerance of residues chosen for the strand segments. Hairpins and sheets are primarily stabilized by cooperative cross-strand hydrogen bonding, with facing residue interactions appearing to be of only marginal importance (31,36). Consequently, β-sheet design appears to have been facilitated by the recognition of the critical role of turn nucleation of appropriate stereochemistry, although early attempts at *de novo* design of β-sheets encountered seemingly intractable problems due to limited solubility and uncontrolled aggregation of designed peptides (3). The use of multiple turn segments, placed appropriately in synthetic sequences can generate intramolecular multistranded sheets. Here, we

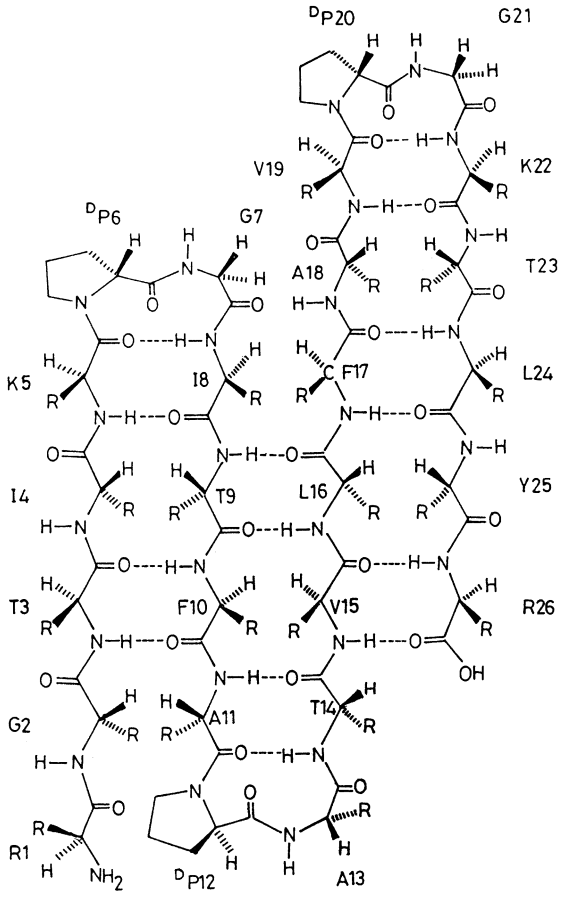

Figure 1. Schematic representation of the proposed structure of Beta-4 with its amino acid sequence. Hydrogen-bonding interactions expected for the antiparallel β-sheet structure are shown by dashed lines connecting the donor and acceptor atoms.

analyze the solution conformations of a designed four-stranded β-sheet structure in a synthetic 26 residue peptide Beta-4 (Fig. 1) (37). Beta-4 contains three internally positioned ^{D}Pro-Xxx segments (6–7, 12–13 and 20–21). The first and the third turn segments have Gly and the middle turn has L-Ala at the '*i*+2' position of the β-turns. The sequence is rich in the β-branched residues Ile, Val and Thr which have a high propensity to adopt extended strand structures (38–40), while the charged residues at the N- and C-termini are selected to prevent aggregation (20). The choice and positioning of the residues was also dictated by the need to have easily detectable cross-strand NOEs between side-chain protons, which could provide ready diagnostics of β-sheet formation. Aromatic residues (Phe and Tyr) have been paired with aliphatic residues across the strands to enable easy identification of interside-chain NOEs. The studies described in this report establish that a stable four-stranded β-sheet is observed in methanol and 50% (v/v) methanol/water solutions. In water, solvent invasion of the strands results in a loss of cross-strand hydrogen bonds, thereby leading to disruption of strand

registry, although the nucleating turns, and hydrophobic clusters expected in the β-sheet remain intact.

Experimental Procedures

Peptide synthesis and purification

Peptide Beta-4 was synthesized using standard solid-phase peptide synthetic methods using Fmoc chemistry (41). The resin assembled peptide was cleaved in 95% trifluoroacetic acid (TFA) containing anisole (2.5%, v/v) and ethane dithiol (2.5%, v/v) as cation scavengers. Purification of the peptide was achieved by reverse phase HPLC on a C18 column (5–10 μ, 7.8×250 mm). A flow rate of 1.5 mL/min was used, with a linear gradient of 5–55% buffer B over 50 min (buffer A: water, 0.1% TFA; buffer B: water 20%, acetonitrile 80%, 0.1% TFA). The purified peptide was analyzed by electrospray mass spectrometry (M_{obs} 2775.1, M_{calc} 2775.3) on an Hewlett Packard 1100 LCMSD mass spectrometer.

NMR spectroscopy

All ^{1}H NMR experiments were performed at 500 MHz on a Bruker DRX500 spectrometer. One-dimensional spectra were acquired using 32 000 data points and processed with 1 Hz line broadening. All chemical shifts in aqueous solutions were referenced to the sodium salt of trimethylsilylpropionate (TSP). The residual methyl resonance in CD_3OH was used as the internal standard for chemical shift referencing (42). All two-dimensional experiments were carried out in the phase-sensitive mode using time proportional phase incrementation. DQF-COSY (43), TOCSY (44), NOESY (45) and ROESY (46,47) experiments were performed collecting 1000 data points in f2 and 512 data points in f1 using a spectral width of 5500 Hz. Solvent suppression was achieved using presaturation (using a 55-dB pulse in a recycle delay of 1.5 s) and watergate sequences with standard pulse sequences available in the Bruker library. Data were processed on a Silicon Graphics Indy work station using Bruker XWINNMR software. Typically, a shifted ($\pi/2$) sine-squared window function was applied in both the dimensions. Data in f1 was zero-filled to 1000 points. Mixing times of 200–300 ms were used in NOESY experiments. A spin lock mixing time of 300 ms was used in ROESY experiments. A 70-ms mixing time was used for TOCSY experiments. The sample concentration was ≈3 mM and the probe temperature was maintained at 300 K.

Structure calculations

A total of 100 observed NOEs in methanol solution was used to derive upper limit distance restraints. NOEs were classified as strong (≤2.5 Å), medium (≤3.5 Å), weak (≤4.5 Å) and very weak (≤5.0 Å) according to their intensities judged by visual inspection of contour levels. The choice of distance limits was based on the expectation that NOEs at distances >5.0 Å are unlikely to be detected in peptides of the size of Beta-4. In addition to NOEs, 11 dihedral restraints from J-values ($^3J_{C\alpha H\text{-}NH}$ values ≥ 8.5 Hz were used to restrain ϕ to -90° to -150°), and 10 hydrogen bonding constraints from H/D exchange data (the hydrogen bonding pairs, C=O....HN, identified are: T3–F10, K5–I8, I8–K5, T9–L16, L16–T9, A11–T14, T14–A11, F17–L24, K22–V19 and L24–F17) were also used as inputs for structure calculations. Simulated annealing using DYANA 1.5 (48) was performed with 30 random starting conformations for 30 000 dynamic steps. Twelve of the resulting structures with the lowest target function values were selected for further analysis. None of these structures violated restraints by >0.2 Å. These structures superpose with a mean RMSD of 0.59 Å, calculated using MOLMOL (49), for all backbone atoms in the well-ordered region of residues 3–25 and 1.32 Å for all heavy atoms in the same region of residues.

Circular dichroism

All CD spectra were recorded on a JASCO J-715 spectropolarimeter. The instrument was calibrated with d(+)-10-camphor sulphonic acid. The path length used was 1 mm with a peptide concentration of ≈ 100 μM. The data were acquired in the wavelength scan mode, using 1-nm band width with a step size of 0.2 nm. Typically, eight scans were acquired from 255 to 190 nm using 50 nm/min scan speed. The resulting data were baseline corrected and smoothed.

Results and Discussion

Molecular conformation in methanol

Beta-4 yields an extremely well-resolved 500 MHz ^{1}H NMR spectrum characterized by sharp resonances. The spectra revealed no significant concentration dependence over the range 0.1–3.2 mM suggesting absence of aggregation effects. The sharp resonances are consistent with a major population of monomeric structures for this 26-residue sequence.

Complete sequence specific assignment of resonances was achieved using a combination of TOCSY experiments to identify individual spin systems and NOESY/ROESY experiments to identify near neighbor connectivities (50). Table 1 summarizes the chemical shifts of all the assigned protons in Beta-4. Large values of coupling constants $^{3}J_{C\alpha H\text{-}NH} \geq 8.5$ Hz are observed for several resonances [J(Hz): T3 (8.9), I4 (4.9), K5 (6.8), F10 (4.9), A11 (9.0), T14 (9.0), A18 (5.8), V19 (6.8), K22 (8.8), L24 (7.8), Y25 (5.8)] which could be measured accurately from a resolution-enhanced one-dimensional spectrum. These values are most consistent with the dihedral angle ϕ occurring in the extended region of the Ramachandran map (51).

An H/D exchange experiment, carried out by dissolving Beta-4 in CD_3OD, revealed that as anticipated the NH resonances of G7, A13 and G21, which are the '*i*+2' residues of the three turns, exchange very rapidly (data not shown). Of the other resonances G2, T3, K22 and R26 exchanged relatively rapidly. G2 is exposed in the expected structure while T3 and R26 groups are close to the termini. The behavior of K22 was anomalous. All other NH groups which are expected to be internally hydrogen bonded exchanged relatively slowly and have exchange half-lives ≥ 4 h. The exposed NH groups on the two outer strands of the β-sheet (I4, T23 and Y25) exchanged relatively slowly. In attempting to rationalize observed H/D exchange rates in terms of the assumed β-sheet structure it is important to note two complicating features: (i) Englander and co-workers clearly established intrinsic variation of exchange rates depending on residue type and mechanism of exchange (52); (ii) in the extended strand conformation the 'outward' facing CO and NH groups of the residues in the nonhydrogen bonding positions are proximate, and the possibilities of C_5 interaction (53) which retards H/D exchange cannot be excluded. Notably, such exposed NH groups some times behave anomalously in other experiments designed to delineate

Table 1. **^{1}H NMR assignments for Beta-4 (CD_3OH, 300 K)**

Residue	HN	H_α	H_β	Others
Arg[1]	–	4.04	1.97, 1.76	H_γ 1.76; H_δ 3.27; NH_δ 7.64
Gly[2]	8.73	4.35, 4.13		
Thr[3]	8.62	4.63	4.18	H_γ 1.22
Ile[4]	8.35	4.85	1.75	CH_3-H_γ 0.93; H_γ 1.25; H_δ 0.93
Lys[5]	9.07	4.85	1.92, 1.82	H_γ 1.46; H_δ 1.82; H_ε 2.95; NH_ε 7.80
^{D}Pro[6]		4.40	2.23, 2.03	H_γ 2.03; H_δ 3.77s
Gly[7]	8.75	4.17, 3.82		
Ile[8]	8.14	4.78	1.87	CH_3-H_γ 0.42; Hγ 0.96, 1.62; H_δ 0.82
Thr[9]	8.71	4.87	3.91	H_γ 1.05
Phe[10]	9.03	5.04	3.14, 3.05	H_δ 7.23; $H_{\varepsilon,}$ Hz 7.17–7.19
Ala[11]	8.78	5.00	1.22	
^{D}Pro[12]		4.43	2.21, 2.03	H_γ 1.98; H_δ 3.55, 3.78
Ala[13]	8.83	4.42	1.48	
Thr[14]	8.19	4.58	4.27	H_γ 1.23
Val[15]	8.13	4.65	1.87	H_γ 0.62, 0.82
Leu[16]	8.75	5.09	1.54, 1.45	H_γ 1.45; H_δ 0.80
Phe[17]	8.73	5.12	2.91, 3.00	H_δ 7.13; $H_{\varepsilon,}$ Hz 7.13–7.19
Ala[18]	8.60	4.97	1.32	
Val[19]	8.50	4.53	2.04	H_γ 0.96
^{D}Pro[20]		4.35	2.27, 2.14	H_γ 2.02; H_δ 3.77
Gly[21]	8.55	3.87		
Lys[22]	8.04	4.62	1.87, 1.69	H_γ 1.50; H_δ 1.69; H_ε 2.95; NH_ε 7.81
Thr[23]	8.14	4.78	3.98	H_γ 1.08
Leu[24]	8.68	4.62	1.48	H_γ 1.48; H_δ 0.89
Tyr[25]	8.27	5.18	2.96	H_δ 7.03; H_ε 6.70
Arg[26]	8.67	4.55	2.00, 1.79	H_γ 1.68; H_δ 3.23; NH_δ 7.42

solvent exposed NH groups, such as solvent-induced perturbation of chemical shifts and radical-induced line broadening (19). Slow exchange of apparently exposed NH groups in β-strands is ascribed to hindrance to solvation due to proximal CO groups. At this stage, the possibility that the anomalous exchange rates in Beta-4 arise from alternative folded conformations cannot be excluded.

Figures 2 and 3 show the NOESY spectra which illustrate the observed $d_{\alpha N}$ ($C^{\alpha}H_i$ NH_{i+1}) and $d_{\alpha\alpha}$ ($C^{\alpha}H_i$ $C^{\alpha}H_j$) connectivities. In extended strands, intense $d_{\alpha N}$ ($C^{\alpha}H_i$ NH_{i+1}) are expected, while the intraresidue $d_{\alpha N}$ ($C^{\alpha}H_i$ NH_i) should be weaker. This is indeed the case in Fig. 2. Cross-strand NOEs between $C^{\alpha}H$ groups distant in sequence are a clear diagnostic of proper registry of strand segments as expected in the antiparallel β-sheet shown in Fig. 1. Indeed, the observation of four distinct $d_{\alpha\alpha}$ connectivities between I8–F17, V10–F15, A18–T23 and L16–Y25 (Fig. 3) are a strong indicator that the four-stranded β-sheet structure is formed, as anticipated in Fig. 1. The observation of the $d_{\alpha\alpha}$ NOE between I4 and T9 was obscured due to overlap of $C^{\alpha}H$ resonances belonging to these residues. In addition, all d_{NN} (N_iH $N_{i+1}H$) NOEs, characteristic of turn conformations at the three potential chain reversal sites, are observed. Strand registry in the antiparallel sheet is expected to bring several NH groups distant in the sequence to proximal distances giving rise to observable NOEs. In the NOESY spectra of Beta-4 several such NOEs (T3–F10, K5–I8, A11–T14, V19–K22 and V15-R26) could be observed lending strong evidence

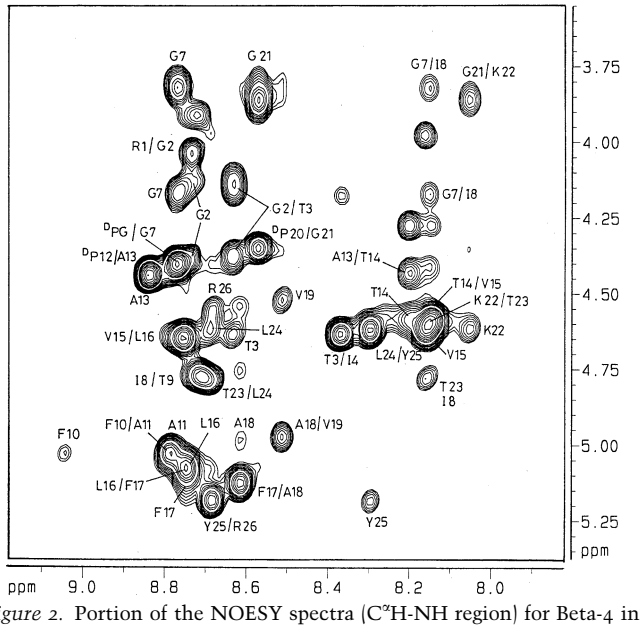

Figure 2. Portion of the NOESY spectra ($C^{\alpha}H$-NH region) for Beta-4 in CD_3OH at 300 K illustrating the observed $d_{\alpha N}$ ($C^{\alpha}H_i$ NH_{i+1} and $C^{\alpha}H_i$ NH_i) interactions. Cross-peaks are annotated with their corresponding residue numbers using one letter code for amino acids.

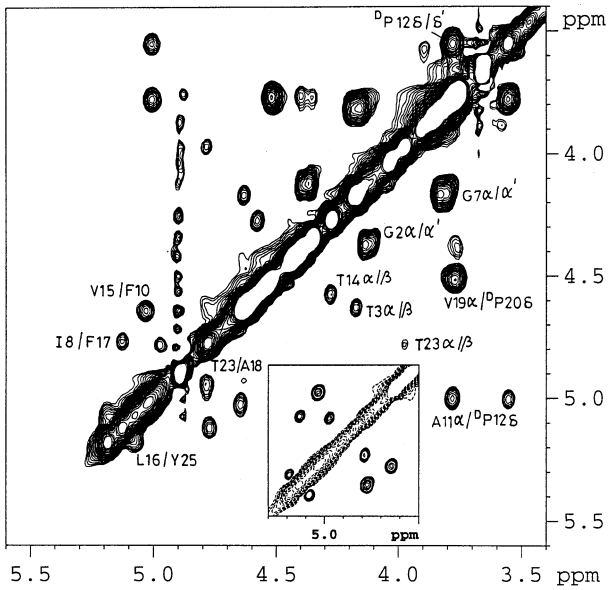

Figure 3. Portion of the NOESY spectra ($C^{\alpha}H$-$C^{\alpha}H$ region) for Beta-4 (CD_3OH) at 300 K showing $d_{\alpha\alpha}$ connectivities. The inset shows portion of the ROESY spectrum of Beta-4 in CD_3OD at 300 K, highlighting interstrand $d_{\alpha\alpha}$ cross-peaks.

for strand alignment in the β-sheet. Other expected d_{NN} NOEs (T9–L16 and F17–L24) could not be observed because of accidental chemical shift degeneracy of these resonances. NOEs between side-chain protons, indicative of their proximity across antiparallel strands were also observed. Most notably, NOEs could be detected between the side-chain protons of T3–F10, I8–F17, V15–F10 and L16–Y25. The NOE between T3 and F10 side-chains is noteworthy since these side-chains are expected to face outwards in a hydrogen-bonded residue pair (Fig. 1). It should be noted that although C^{α} and C^{β} bonds project outwards appropriate values of χ^1 and χ^2 can bring the F10 ring protons and T3 $C^{\gamma}H_3$ protons to distances observable by NOE. Similar NOEs have also been detected between the side-chains of hydrogen-bonded residue pairs in other β-hairpin and β-sheet structures in designed sequences (20,26). The observed NOEs provide conclusive evidence of extensive side-chain interactions in the β-sheet. Using a total of 100 observed NOEs, 11 dihedral angles and 10 hydrogen-bonding restraints a family of four-stranded β-sheet structures compatible with the NMR data could be generated. Of these, 12 structures with lowest energy values were selected that did not violate the distance restraints beyond 0.2 Å. The RMSD between these structures is 0.59 Å for the backbone atoms in the region of residues 3–25 and 1.32 Å for all heavy atoms in the same region of residues [calculated using MOLMOL (49)]. Figure 4 shows a superposition of 7 such calculated structures represented as a ribbon drawing. The nonpolar cluster formed by I8, F10, V15 and F17 in strands 2

and 3 is highlighted. Calculations carried out by increasing the number of random starting conformations did not change the nature of the calculated structures significantly. Structure calculations were also carried out in the absence of 10 hydrogen-bonding restraints resulting in convergence to a close-related family of four-stranded β-sheet structures, albeit with larger deviations between the members of the family and a poorly defined N-terminal strand (RMSD between 10 best structures is 1.17 Å for the backbone atoms in the region of residues 3–25 and 1.85 Å for all heavy atoms in the same region). A notable feature is that the sequential NH-NH NOEs which are indicative of a population of nonβ-sheet conformations are very weak or absent, suggesting that Beta-4 folds predominantly into the four-stranded structure. The quantitation of the extent of folded structure in designed peptides is a difficult proposition at present (54).

Conformations in 50% methanol/water and water

The observation of a well-defined four-stranded β-sheet structure in the peptide Beta-4 prompted us to investigate the stability of this fold in water and mixed methanol/water systems. Because the four-stranded β-sheet is stabilized primarily by cooperative cross-strand hydrogen bonds it might be expected that in a strongly hydrogen bonding solvent, such as water, solvation forces may result in disruption of strand registry. In both these solvent systems, Beta-4 yielded well-resolved NMR spectra with sharp resonances, as in the case of methanol. Complete assignment of all proton resonances was accomplished in both 50% methanol/water and water (pH 3.7), as described earlier for methanol. Figure 5 shows the chemical shifts of the $C^{\alpha}H$ protons of Beta-4 referenced to random coil chemical shifts (55). It is clearly seen that in methanol most of the $C^{\alpha}H$ resonances of the strand residues are significantly shifted to lower field, a feature characteristic of a β-sheet conformation (56). Indeed, the four strands and three turn segments can be clearly identified from the chemical shift values. In 50% methanol/water, delineation of the strand segments on the basis of $C^{\alpha}H$ chemical shifts is still possible, although some resonances now move to higher field positions, indicative of conformational changes and averaging. In H_2O at pH 3.7 there is a significant loss of dispersion of $C^{\alpha}H$ chemical shifts and appreciable upfield shift of $C^{\alpha}H$ protons. The low field positions of $C^{\alpha}H$ groups belonging to several residues immediately flanking the turn segments is noteworthy, and may indicate the retention of well-defined structures in these regions. A characteristic feature of the Beta-4 conformation in methanol is the nonpolar cluster involving residues I8, F10, V15 and F17. A consequence of this structure is the high field position of the methyl resonances of I8 and V15 due to the ring current of proximal aromatic residues. Figure 6 shows the methyl resonances of Beta-4 in three solvent systems. The effects of aromatic ring currents appear to be retained, albeit to a lesser extent in 50% methanol/water and water (pH 3.7), suggesting that that the nonpolar cluster is maintained even in a completely aqueous medium. A crucial piece of evidence for the stability of the cluster is obtained from the observation of interresidue side-chain NOEs. The inset in Fig. 6 shows the NOEs between methyl protons of I8 and V15 in 50% methanol/water solutions. Figure 7 shows the interside-chain NOEs observed for Beta-4 in the three solvent systems. Inspection of the side-chain NOEs suggests that almost all the NOEs observed in methanol are retained in 50% methanol/water. There is a clear loss of interstrand tertiary NOEs in water. The four-stranded β-sheet structure in methanol is characterized by observation of several cross-strand NH-NH NOEs and sequential NH-NH NOEs at the three turn segments as shown in Fig. 8. Once again the NOEs are also largely retained in 50% methanol/water solution. In water, almost all the cross-strand NH-NH NOEs are lost but the sequential connectivities of the three turn segments G7–I8, A13–T14 and G21–K22 are retained. NMR studies suggest that the four-stranded β-sheet structure in Beta-4 is largely retained in a 50% methanol/water mixture. In water, the NMR evidence suggests that the turn segments retain their structural integrity, but all the cross-strand registry is lost, presumably due to solvent invasion of the backbone.

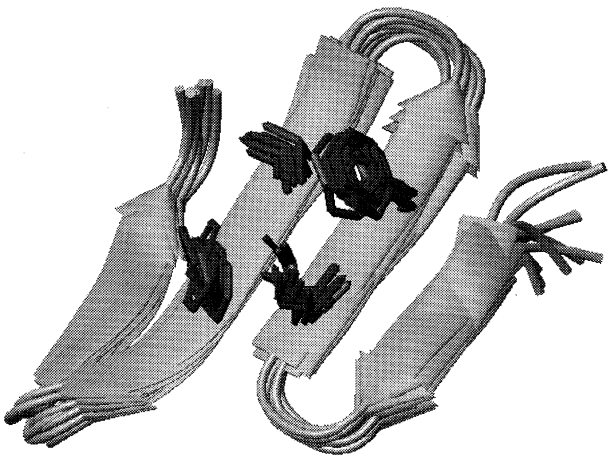

Figure 4. Ribbon representation of seven superposed structures [calculated using DYANA (48)] of Beta-4 derived from NMR restraints. The nonpolar cluster involving I8, F10, V15 and F17 side-chains is highlighted. The figure was generated using MOLMOL (49).

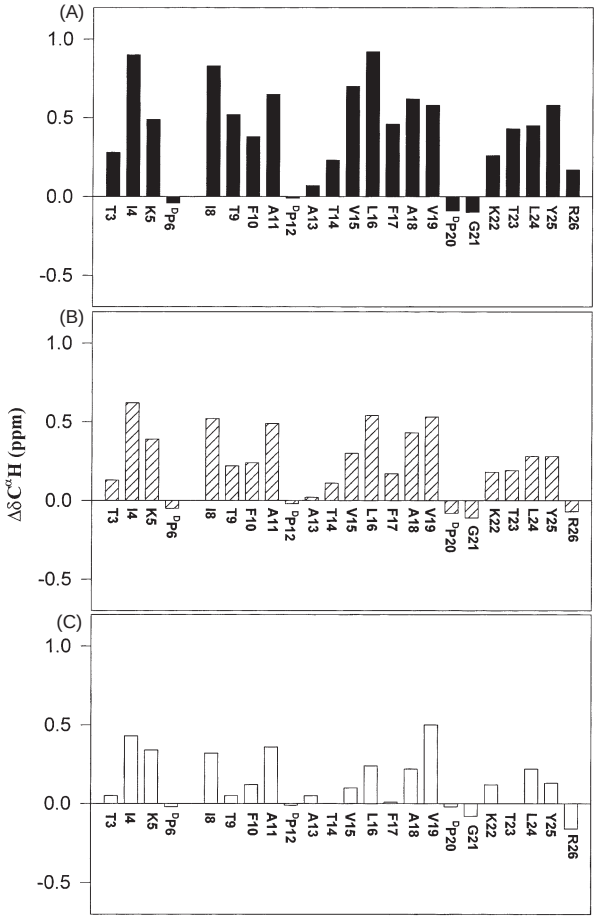

Figure 5. Conformational shifts for the peptide Beta-4 in the region T3-R26. ΔδC$^{\alpha}$H (p.p.m.) is the deviation of chemical shifts of C$^{\alpha}$H protons from their random coil values (observed $\delta_{C\alpha H}$ – random coil $\delta_{C\alpha H}$) in (A) CD_3OH at 300 K; (B) 50% (v/v) aqueous methanol at 300 K; and (C) water (pH 3.7) at 300 K. For random coil values see Ref. 55. No data are shown for Gly^7 because there are two C$^{\alpha}$H resonances in most cases.

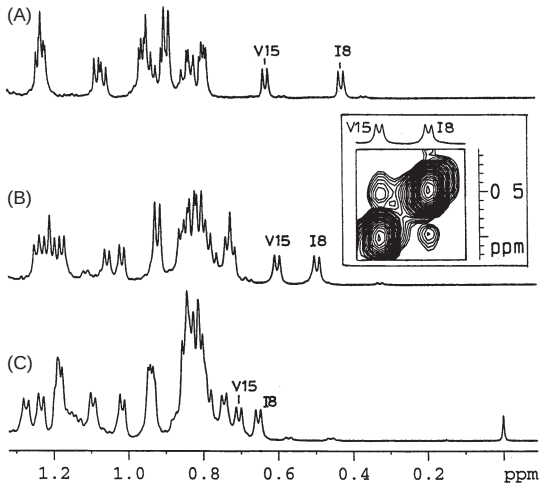

Figure 6. Portions of one-dimensional spectra of Beta-4 in (A) CD_3OH (300 K); (B) 50% (v/v) aqueous methanol (300 K); and (C) water (pH 3.7, 300 K). The inset illustrates NOE observed between the methyl groups of I8 and V15 at the solvent composition of 50% methanol/water (v/v).

Circular dichroism

Figure 9 shows the CD spectra of Beta-4 in methanol, water and methanol/water mixtures. In methanol, the peptide shows a strong negative band at 215 nm and a positive band at 198 nm, which resemble the CD spectra expected for classical β-sheet structures (57). A negative long wavelength shoulder at 225–227 nm is also observed. The CD spectra arising from the electronic transition associated with the peptide backbone (n-π*, π-π*) do not normally yield bands at wavelengths >225 nm in large peptides. We assign this longwave length shoulder to the contribution from two Phe and one Tyr residues present in the sequence. Aromatic contributions to the far-UV CD have been widely recognized (58,59). Indeed, in short β-hairpin peptides containing Phe residues which face each other across strands, we have observed anomalous far-UV CD spectra in the region below 230 nm (60). The alternate possibility that the long wavelength shoulder may arise from a contribution due to a population of helical structures has been excluded because of the absence of a significant shoulder below 210 nm and also because the NMR data do not show significant intensity for sequential N_iH-$N_{i+1}H$ NOEs, which are generally characteristic of helical structure. The presence of as many as three ^{D}Pro residues (positions 6, 12 and 20) in the sequence also precludes the development of helical segments of any significant length. Addition of water results in a steady loss of ellipticity of both the negative and positive bands at 215 and 198 nm, respectively. Significant intensities characteristic of β-sheet conformations are observed at a 50% methanol/water composition. A noteworthy feature of the CD studies is that even in a 70% water/methanol mixture, the negative CD band at 215 nm and the positive band at 198 nm are detectable, suggesting that a significant population of β-sheet conformations is present under these conditions.

Together with NMR studies, the CD results suggest that the well-formed β-sheet structure in methanol melts to a poorly organized, 'unfolded' state in water. The gradual loss of ellipticity with increasing concentration of water (Fig. 9, inset) suggests the absence of a well-defined cooperative transition from a folded to an unfolded state. The lack of well-defined structural transitions in designed peptides has also been noted in other synthetic motifs (61,62). The difficulties in using designed hairpins as models for studies regarding folding and unfolding transitions has also been discussed (54). It is particularly important to note that the

quantitation of folded structures from CD band intensities is an extremely risky proposition (54). In these studies the use of NOE in conjunction with CD suggests that the peptide Beta-4 is indeed disorganized in water.

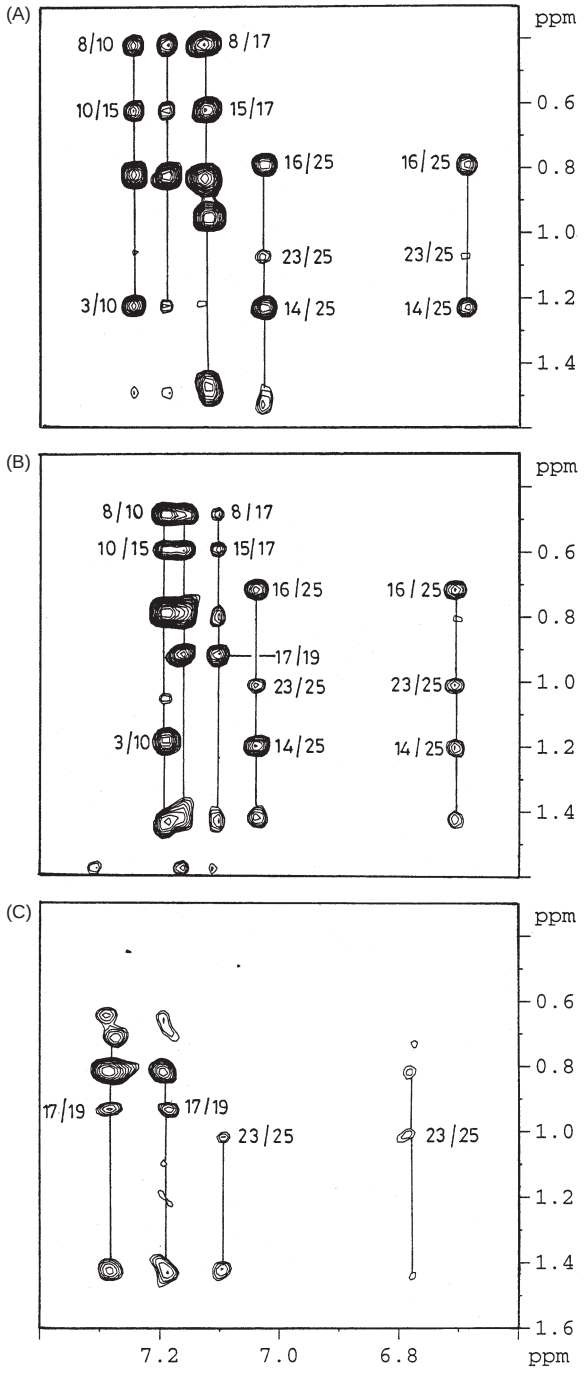

Figure 7. Comparison of a portion of NOESY spectra of Beta-4 relating aromatic ring protons of F10, F17 and Y25 with those of methyl groups from aliphatic residues in (A) CD_3OH (300 K); (B) 50% (v/v) aqueous methanol (300 K) and (C) water (pH 3.7, 300 K). Important long-range NOEs diagnostic of the β-sheet structure are annotated with their corresponding residue numbers.

Effect of temperature on Beta-4 in water

We attempted to investigate whether the β-sheet conformation could be populated in water by carrying out low-temperature NMR and CD studies. Figure 10 shows the effect of temperature on the high field methyl resonance of Beta-4. At 350 K no anomalously shifted resonances due to I8 and V15 are observed. Upon cooling, there is an upfield movement of V15 and I8 methyl resonances, indicating an ordering of side-chains of the nonpolar cluster formed by

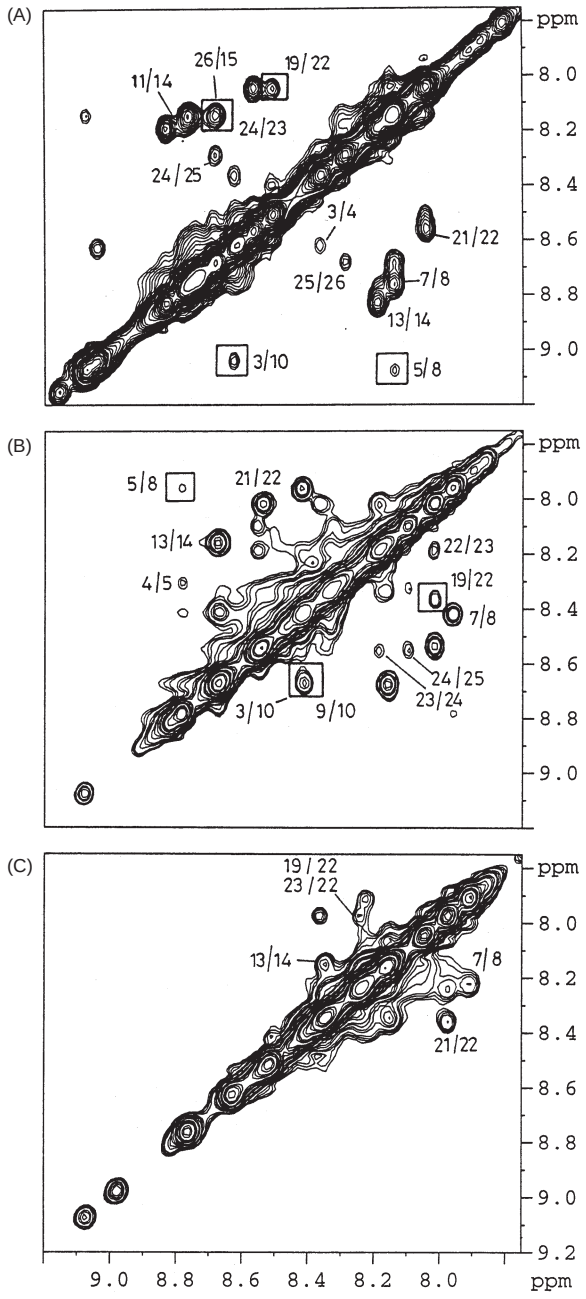

Figure 8. Comparison of a portion of NOESY spectra (NH-NH region) of Beta-4 in (A) CD_3OH (300 K); (B) 50% (v/v) aqueous methanol (300 K) and (C) water (pH 3.7, 300 K). Important long-range NOEs are boxed.

side-chains on strands 2 and 3. Interestingly, below 290 K there appears to be no further change in the chemical shifts of these resonances, the observed values being significantly lower field than in pure methanol. Even at low temperature (277 K) no significant change in the pattern of NOEs was observed. These results suggest that while residual structures involving formation of a nonpolar cluster may be stabilized at low temperature, there is no evidence for a well-formed β-sheet in water.

Conclusions

These studies establish that peptide design strategies can be extended to the construction of multistranded β-sheets using internally positioned ^{D}Pro-Xxx sequences for hairpin nucleation. The peptide Beta-4 folds predominantly into the expected four-stranded β-sheet conformation in methanol. NOE data are consistent with a major population of structures in which the three ^{D}Pro-Xxx β-turns are formed, resulting in appropriate strand registry. In peptide Beta-4 most NH and CO groups are internally hydrogen bonded resulting in excellent solubility in both water and alcohols. Solvation of the edge strands and positioning of charged residues at the N and C-termini limits aggregation by preventing formation of 'open' sheet structures. The four-stranded β-sheet structure loses its integrity in aqueous solution. The fragility of the intramolecular β-sheet in water is undoubtedly a consequence of solvent competition for interstrand hydrogen bonds, which appear to be the dominant structure stabilizing interaction in the present case. In proteins, most β-sheets are well shielded from the aqueous environment. The stabilization of sheets in water may be achieved by interstrand cross-linking using disulfide bridges and possibly by increasing the number of strands and their length. Although the principle thrust of attempts at *de novo* designed β-sheet structures is directed towards stabilizing the structures in aqueous solution, the significance of the formation of well-characterized multistranded sheets in methanol must be emphasized. Several membrane proteins consist of β-sheet domains which span the low-dielectric environment of phospholipid membranes. A noteworthy feature of β-sheets is their tendency to curve (63). Indeed, the growing family of transmembrane proteins which adopt β-barrel structures, best exemplified by porins (64), suggests that closed barrels may be one of the most efficient ways to traverse the lipid bilayer (65). *De novo* design of β-barrel structures now appears to be a real possibility because of the automatic curvature generated by multistranded β-sheets, which should eventually induce the

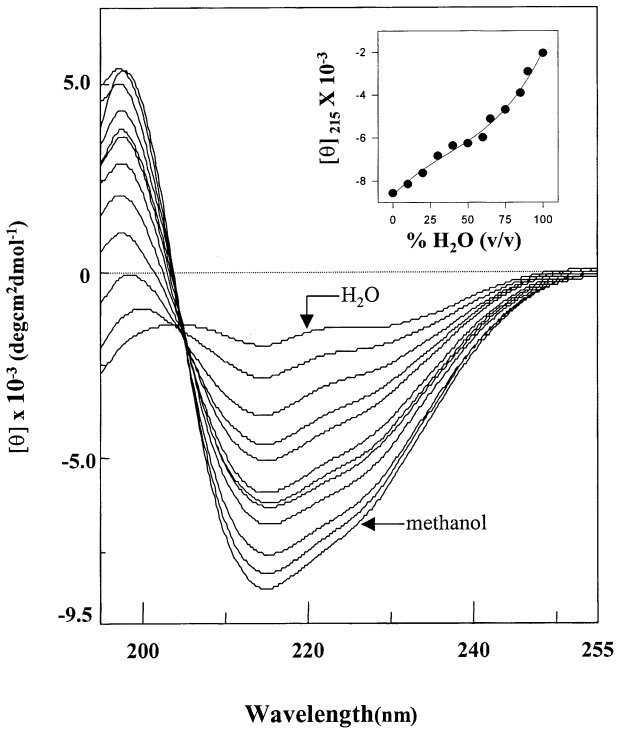

Figure 9. Far-UV CD spectra ([θ] is the mean residue ellipticity) of Beta-4 in various compositions of methanol and water at 300 K. The spectra in water (pH 3.7) and methanol are marked. The 10 intermediate spectra correspond to solvent composition (% v/v) of methanol/water 10:90, 20:80, 30:70, 40:60, 50:50, 60:40, 65:35, 75:25, 85:15 and 90:10. The inset illustrates the variation of mean residue ellipticity as a function of increasing amount of water content in methanol.

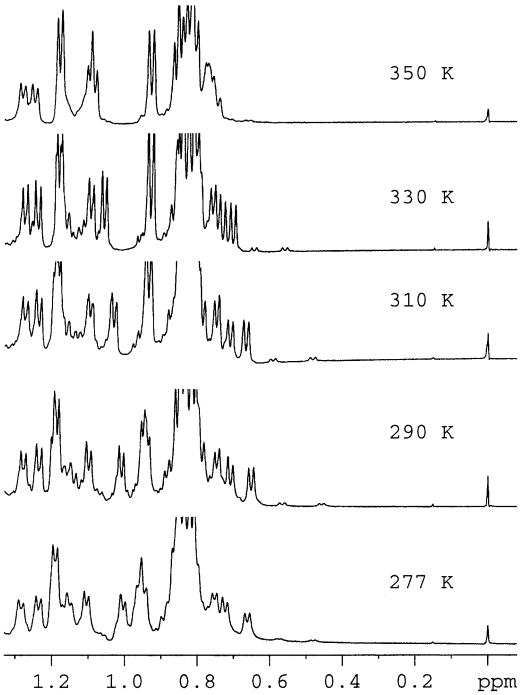

Figure 10. Variation of high field resonances of Beta-4 in water (pH 3.7) with temperature.

structure to fold upon itself. β-Sheets lend themselves to ready synthetic construction because of the relatively simple principle involved in the generation of the structural motif.

Acknowledgments: The authors thank Dr David Cowburn (Rockefeller University) for his advice on including the D-Pro residue into the DYANA library. Program support for the area 'Drug and Molecular Design' by the Department of Biotechnology, Government of India is gratefully acknowledged.

References

1. DeGrado, W.F., Summa, C.M., Pavone, V., Nastri, F. & Lombardi, A. (1999) *De novo* design and structural characterization of proteins and metalloproteins. *Annu. Rev. Biochem.* **68**, 779–819.
2. Betz, S.F., Bryson, J.W. & DeGrado, W.F. (1995) Native-like and structurally characterized designed α-helical bundles. *Curr. Opin. Struct. Biol.* **5**, 457–463.
3. Richardson, J.S., Richardson, D.C., Tweedy, N.B., Gernert, K.M., Quinn, T.P., Hecht, M.H., Erickson, B.W., Yan, Y., McClain, R.D., Donlan, M.E. & Surles, M.C. (1992) Looking at proteins: repesentations, folding, packing and design. *Biophys. J.* **63**, 1186–1209.
4. Quinn, T.P., Tweedy, N.B., Williams, R.W., Richardson, J.S. & Richardson, D.C. (1994) Beta-doublet: *de novo* design, synthesis, and characterization of a β-sandwich protein. *Proc. Natl Acad. Sci. USA* **91**, 8747–8751.
5. Smith, C.K. & Regan, L. (1997) Construction and design of β-sheets. *Acc. Chem. Res.* **30**, 153–161.
6. Yan, Y. & Erickson, B.W. (1994) Engineering of betabellin 14D: disulfide-induced folding of a β-sheet protein. *Protein Sci.* **3**, 1069–1073.
7. Hill, R.B. & DeGrado, W.F. (1998) Solution structure of α_2D, a nativelike *de novo* designed protein. *J. Am. Chem. Soc.* **120**, 1138–1145.
8. Struthers, M.D., Cheng, R.P. & Imperiali, B. (1996) Design of a monomeric 23-residue polypeptide with defined tertiary structure. *Science* **271**, 342–345.
9. Dahiyat, B.I. & Mayo, S.L. (1997) *De novo* protein design: fully automated sequence selection. *Science* **278**, 82–87.
10. Rohl, C.A. & Baldwin, R.L. (1998) Deciphering rules of helix stability. *Methods Enzymol.* **295**, 1–26.
11. Walsh, S.T.R., Cheng, H., Bryson, J.W., Roder, H. & DeGrado, W.F. (1999) Solution structure and dynamics of a *de novo* designed three-helix bundle protein. *Proc. Natl Acad. Sci. USA* **96**, 5486–5491.
12. Johansson, J.S., Gibney, B.R., Skalicky, J.J., Wand, A.J. & Dutton, P.L. (1998) A native-like three-α-helix bundle protein from structure-based redesign: a novel maquette scaffold. *J. Am. Chem. Soc.* **120**, 3881–3886.
13. Brive, L., Dolphin, G.T. & Baltzer, L. (1997) Structure and function of an aromatic ensemble that restricts the dynamics of the hydrophobic core of designed helix-loop-helix dimer. *J. Am. Chem. Soc.* **119**, 8598–8607.
14. Schafmeister, C.E., LaPorte, S.L., Miercke, J.W. & Stroud, R.M. (1997) A designed four helix bundle protein with native-like structure. *Nature Struct. Biol.* **4**, 1039–1046.
15. Haque, T.S., Little, J.C. & Gellman, S.H. (1996) Stereochemical requirements for β-hairpin formation: model studies with four-residue peptides and depsipeptides. *J. Am. Chem. Soc.* **118**, 6975–6985.
16. Haque, T.S. & Gellman, S.H. (1997) Insights on β-hairpin stability in aqueous solution from peptides with enforced type I′ and type II′ β-turns. *J. Am. Chem. Soc.* **119**, 2303–2304.
17. Awasthi, S.K., Raghothama, S. & Balaram, P. (1995) A designed β-hairpin peptide. *Biochem. Biophys. Res. Commun.* **216**, 375–381.
18. Karle, I.L., Awasthi, S.K. & Balaram, P. (1996) A designed β-hairpin peptide in crystals. *Proc. Natl Acad. Sci. USA* **93**, 8189–8193.
19. Raghothama, S.R., Awasthi, S.K. & Balaram, P. (1998) β-Hairpin nucleation by Pro-Gly β-turns. Comparison of D-Pro-Gly and L-Pro-Gly sequences in an apolar octapeptide. *J. Chem. Soc., Perkin Trans.* **2**, 137–143.
20. Ramirez-Alvarado, M., Blanco, F.J. & Serrano, L. (1996) *De novo* design and structural analysis of a model β-hairpin system. *Nature Struct. Biol.* **3**, 604–612.
21. De Alba, E., Jimenez, M.A., Rico, M. & Nieto, J.L. (1996) Conformational investigation of designed short linear peptides able to fold into β-hairpin structures in aqueous solution. *Folding Design* **1**, 133–144.
22. De Alba, E., Rico, M. & Jimenez, M.A. (1997) Cross-strand side-chain interactions versus turn conformation in β-hairpins. *Protein Sci.* **6**, 2548–2560.
23. Maynard, A.J., Sharman, G.J. & Searle, M.S. (1998) Origin of β-hairpin stability in solution: structural and thermodynamic analysis of the folding of a model peptide supports hydrophobic stabilization in water. *J. Am. Chem. Soc.* **120**, 1996–2007.
24. Kortemme, T., Ramirez-Alvarado, M. & Serrano, L. (1998) Design of a 20-amino acid three-stranded beta-sheet protein. *Science* **281**, 253–256.
25. Schenck, H.L. & Gellman, S.H. (1998) Use of a designed triple-stranded antiparallel β-sheet to probe β-sheet cooperativity in aqueous solution. *J. Am. Chem. Soc.* **120**, 4869–4870.
26. Sharman, G.J. & Searle, M.S. (1998) Cooperative interaction between the three strands of a designed antiparallel β-sheet. *J. Am. Chem. Soc.* **120**, 5291–5300.
27. Das, C., Raghothama, S. & Balaram, P. (1998) A designed three-stranded β-sheet peptide as a multiple β-hairpin model. *J. Am. Chem. Soc.* **120**, 5812–5813.
28. De Alba, E., Santoro, J., Rico, M. & Jimenez, M.A. (1999) *De novo* design of a monomeric three-stranded antiparallel β-sheet. *Protein Sci.* **8**, 854–865.
29. Sibanda, B.L. & Thornton, J.M. (1985) β-Hairpin families in globular proteins. *Nature* **316**, 170–174.
30. Sibanda, B.L., Blundell, T.L. & Thornton, J.M. (1989) Conformation of β-hairpins in protein structures. *J. Mol. Biol.* **206**, 759–777.
31. Gunasekaran, K., Ramakrishnan, C. & Balaram, P. (1997) β-Hairpins in proteins revisited: lessons for *de novo* design. *Protein Eng.* **10**, 1131–1141.
32. IUPAC-IUB Commission on Biochemical Nomenclature (*1970) Biochemistry* **9**, 3471–3479.
33. Richardson, J.S. (1981) The anatomy and taxonomy of protein structures. *Adv. Protein Chem.* **34**, 167–330.
34. Srinivasan, N., Anuradha, V.S., Ramakrishnan C., Sowdhamini, R. & Balaram, P. (1994) Conformational characteristics of aspariginyl residues in proteins. *Int. J. Peptide Protein Res.* **44**, 112–122.
35. Stanger, H.E. & Gellman, S.H. (1998) Rules for antiparallel β-sheet design: D-Pro-Gly is superior to L-Asn-Gly for β-hairpin nucleation. *J. Am. Chem. Soc.* **120**, 4236–4237.

36. Wouters, M.A. & Curmi, P.M.G. (1995) An analysis of sidechain interactions and pair correlations within antiparallel beta-sheets: the differences backbone hydrogen-boned and non-hydrogen-bonded residue pairs. *Proteins: Struct. Funct. Genet.* **22**, 119–131.
37. Das, C., Raghothama, S. & Balaram, P. (1999) A four stranded β-sheet structure in a designed, synthetic polypeptide. *J. Chem. Soc. Chem. Commun.* 967–968.
38. Kim, C.A. & Berg, J.M. (1993) Thermodynamic beta-sheet propensities measured using a zinc-finger host peptide. *Nature* **362**, 267–270.
39. Smith, C.K., Withika, J., M. & Regan, (1994) A thermodynamic scale of the beta-sheet forming tendencies of the amino acids. *Biochemistry* **33**, 5510–5517.
40. Minor, D.L. Jr P.S.Kim (1994) Measurement of the beta-sheet-forming propensities of the amino acids. *Nature* **367**, 660–663.
41. Atherton, E. & Sheppard, R.C. (1989). *Solid Phase Peptide Synthesis: A Practical Approach.* IRL Press, Oxford.
42. Gottlieb, H.E., Kotlyar, V. & Nudelman, A. (1997) NMR chemical shifts of common laboratory solvents as trace impurities. *J. Org. Chem.* **62**, 7512–7515.
43. Piantini, U., Sorensen, O.W. & Ernst, R.R. (1982) Multiple quantum filters for elucidating NMR coupling networks. *J. Am. Chem. Soc.* **104**, 6800–6801.
44. Braunschweiler, L. & Ernst, R.R. (1983) Coherence transfer by isotropic mixing: application to proton correlation spectroscopy. *J. Magn. Reson.* **53**, 521–528.
45. Kumar, A., Ernst, R.R. & Wüthrich, K. (1980) A two-dimensional nuclear Overhauser enhancement (2D NOE) experiment for the elucidation of complete proton–proton cross-relaxation networks in biological macromolecules. *Biochem. Biophys. Res. Commun.* **95**, 1–6.
46. Bax, A. & Davis, D.G. (1985) Practical aspects of two-dimensional transverse NOE spectroscopy. *J. Magn. Reson.* **63**, 207–213.
47. Bothner-By, A.A., Stephens, R.L., Lee, J., Warren, C.D. & Jeanloz, R.W. (1984) Structure determination of a tetrasaccharide: transient nuclear Overhauser effects in the rotating frame. *J. Am. Chem. Soc.* **106**, 811–812.
48. Güntert, P., Mumenthaler, C. & Wüthrich, K. (1997) Torsion angle dynamics for NMR structure calculation with the new program DYANA. *J. Mol. Biol.* **273**, 283–298.
49. Koradi, R., Billeter, M. & Wüthrich, K. (1996) MOLMOL: a program for display and analysis of macromolecular structures. *J. Mol. Graphics* **14**, 51–55.
50. Wüthrich, K. (1986). *NMR of Proteins and Nucleic Acids.* John Wiley, New York.
51. Pardi, A., Billeter, M. & Wüthrich, K. (1984) Calibration of the angular dependence of the amide proton-C^{α} proton coupling constants, $^{3}J_{HN\alpha}$, in a globular protein. *J. Mol. Biol.* **180**, 741–751.
52. Englander, S.W. & Kallenbach, N.R. (1984) Hydrogen exchange and structural dynamics of proteins and nucleic acids. *Q. Rev. Biophys.* **16**, 521–655.
53. Benedetti, E. & Toniolo, C. (1996) Polypeptide restricted backbone conformation. In *Polymeric Materials Encyclopedia*, Vol. 8 (Salamone, J.C., ed.). CRC Press, Boca Raton, FL, pp. 6472–6481.
54. Lacroix, E., Kortemme, T., de la Paz, M.L. & Serrano, L. (1999) The design of linear peptides that fold as monomeric β-sheet structures. *Curr. Opin. Struct. Biol.* **9**, 487–493.
55. Wishart, D.S., Sykes, B.D. & Richards, F.M. (1992) The chemical shift index: a fast and simple method for the assignment of protein secondary structure through NMR spectroscopy. *Biochemistry* **31**, 1647–1651.
56. Wishart, D.S., Sykes, B.D. & Richards, F.M. (1991) Relationship between nuclear magnetic resonance chemical shift and protein secondary structure. *J. Mol. Biol.* **222**, 311–333.
57. Woody, R.W. (1985) In *The Peptides*, **Vol. 7** (Udenfriend, S., Meienhofer, J., & &.Hruby, V.J., eds). Academic Press, New York, pp. 15–114.
58. Sreerama, N., Manning, M.C., Powers, M.E., Zhang, J., Goldenberg, D.P. & Woody R.W. (1999) Tyrosine, phenylalanine, and disulfide contributions to the circular dichroism of proteins: circular dichroism spectra of wild-type and mutant bovine pancreatic trypsin inhibitor. *Biochemistry* **38**, 10814–10822.
59. Chakrabartty, A., Kortemme, T., Padmanabhan, S. & Baldwin, R.L. (1993) Aromatic side-chain contribution to far-ultraviolet circular dichroism of helical peptides and its effect on measurement of helix propensities. *Biochemistry* **32**, 5560–5565.
60. Zhao, C., Polavarapu, P.L., Das, C. & Balaram, P. (2000) Vibrational circular dichroism of β-hairpin peptides. *J. Am. Chem. Soc.* in press.
61. Hecht, M.H., Richardson, J.S., Richardson, D.C. & Ogden, R.C. (1990) *De novo* design, expression, and characterization of felix: a four-helix bundle protein of native-like sequence. *Science* **249**, 884–891.
62. Struthers, M.D., Cheng, R.P. & Imperiali, B. (1996) Economy in protein design: evolution of a metal-independent ββα motif based on the zinc finger domains. *J. Am. Chem. Soc.* **118**, 3073–3081.
63. Murzin, A.G., Lesk, A.M. & Chothia, C. (1994) Principles determining the structure of β-sheet barrels in protens. II. The observed structures. *J. Mol. Biol.* **236**, 1382–1400.
64. Schulz, G.E. (1996) Porins: general to specific, native to engineered passive pores. *Curr. Opin. Struct. Biol.* **6**, 485–490.
65. Buchanan, S.K. (1999) β-Barrel proteins from bacterial outer membranes: structure, function and refolding. *Curr. Opin. Struct. Biol.* **9**, 455–461.